https://ijpb.ui.ac.ir/?lang=en

Journal of Plant Biological Sciences
E-ISSN: 3041-9603
Vol. 17, No. 66, 2025, pp. 1- 14
Received: 2025/05/27 Accepted: 2025/09/24

(Research Paper)

Effects of industrial water pollution on morphological, anatomical, and male reproductive characteristics of *Suaeda maritima*

Narges Sadat Mohammadi[1]*, Parissa Jonoubi[2], Ahmad Majd[2], Mansoureh Dehghani[3]

[1] Department of Biology, Zand Institute of Higher Education, Shiraz, Iran.
[2] Department of Plant Sciences, Faculty of Biological Sciences, Kharazmi University, Tehran, Iran.

[3] Research Center for Health Sciences, Department of Environmental Health, School of Health, Shiraz University of Medical Sciences, Shiraz, Iran

Abstract

Suaeda maritima L. Dumort is one of the most resistant halophyte plants. The purpose of this study was to investigate structural changes in *S. maritima* and alterations in morphology under wastewater contamination. Very young seedlings of *S. maritima* were sampled from their natural habitat and treated with tap water and industrial wastewater as the control and treatment, for three months. Then, the plant organs were fixed in FAA fixative and submitted to microtome sectioning, staining, and observation by light microscopy. The Stereolite software quantified the observation. Results showed that the polluted plants were paler in color, had sparse leaves during the vegetative phase, and had a delayed reproductive phase. Root compared to control. These included cell disorders and abnormalities, as well as the changes in cell sizes, tissue layer thicknesses in the stem and root, and cell density. In reproductive organs of the treated plants, changes were observed in the number, size, and shape of pollen grains and the thickness of the anther endocardium layer. The study concluded that industrial wastewater can affect plant morphology and reproductive traits, potentially impairing the spread of the next generation.

Keywords: Anatomical structure; Microsporogenesis; Heavy metals; Wastewater treatment

*Corresponding author: n.mohammadi@zand.ac.ir

doi: 10.22108/IJPB.2025.145310.1411

Introduction

Halophytes are resistant to severe abiotic stresses such as salinity. Most of them are considered phytoremediators because they can accumulate heavy metal pollutants in soil and water (Mohammadi Jahromi et al., 2019a). Studies show that abiotic stress, such as heavy metal pollution, may lead to several structural modifications in both sensitive and resistant plants. For instance, Jesus et al. (2016) found that Al can alter the structure of sunflower leaves and roots. In fact, a wide range of structural and anatomic changes have been observed in plants under abiotic stresses, including an increase in hypodermis thickness, the pith cells' area, and diameter of the stem (Parida et al. 2016), bulliform cells in leaves, aerenchyma in roots, decreased root cortex, and increased sclerenchyma (Hameed et al., 2010).

Suaeda can repair saline-alkali land and protect the environment, promoting agriculture and tourism. Salinization and heavy metal pollution, particularly in coastal and arid areas, are significant environmental issues worldwide (Wang et al., 2022). *Suaeda salsa* plants increase leaf succulence under high salinity by increasing leaf water content and enlarging epidermal cell size (Zhang et al., 2024). Phytoremediation, a low-cost, non-invasive method, utilizes halophytes such as Suaeda to remediate heavy metal-polluted saline soil due to their high tolerance to heavy metals (Wang et al., 2022).

In an attempt to adapt to severe stress conditions, halophytes can modify gene expression, leading to variations in enzyme and metabolite patterns (Koyro et al., 2008). The strategies that help halophytes tolerate salinity include regulation of leaf gas exchange, osmotic regulation, selective ion uptake and transport, exclusion of NaCl from the cytoplasm, and enhanced osmolyte production (Marschner, 1995; Debez et al., 2006; Megdiche et al., 2007). *S. maritima* has been studied for its phytoremediation potential, specifically highlighting its ability to phytoextract heavy metals (Fatnani et al., 2023).

Halophytes also exhibit morphological adaptations. The succulent organs, characterized by large numbers of thin-walled cells, prevent water loss. Halophytes typically have reduced leaves and unusual organ structures with sclerified, resistant parts and polycambial systems, which protect lateral meristems from potential damage (Butnik et al., 2001). Moreover, glandular cells and/or bladder hairs are used to remove salt; reflexive surfaces via wax or trichomes; waxy cuticles; reduced leaves; and high-density, small, sunken stomata are among morphological adaptations that help halophytes resist severe stress conditions (Koyro, 2002).

Heavy metals can modify some anatomical and physiological characteristics in plants. For instance, Mn increases the number of hypodermal cell layers in the stem of *Trapa natans* (Petrovic et al., 2021). Cd stress significantly decreases growth, height, branch number, total leaf area, and shoot dry weight in soybean plants (Pandey et al., 2022). Another study showed that growth and photosynthetic processes in *P. divaricata* were inhibited by a high concentration of Cd, leading to a gradual increase in Fe concentration in the leaves. It also reduces stomatal density, which affects photosynthetic rate (Hu et al., 2023).

Suaeda maritima L. Dumort., of the Amaranthaceae, is a yellow-green shrub with fleshy succulent leaves and tiny flowers. It is a highly resistant species that can accumulate up to 400 mM NaCl in its leaves without significant damage (Wang et al., 2007). The plant is also considered as a hyperaccumulator, capable of storing high concentrations of heavy metals, such as As, Co, Zn, and Cu in its shoots (Mohammadi Jahromi et al., 2019a). While there are some studies on other cultivars of this species, e.g., *Suaeda* spp., the anatomical changes in S. maritima under abiotic stresses are a less-researched area. In fact, few studies have addressed the vegetative growth and reproductive development of *S. maritima* irrigated with industrial wastewater. Therefore, the present study describes the morphology and anatomy of *S. maritima* and reports an investigation into the structural modifications in this halophyte under irrigation with industrial wastewater containing heavy metal pollutants.

Material and Methods

Very young *S. maritima* plants at the early seedling stage, growing in their natural habitat in the experimental area of the Industrial Park Refinery in Shiraz, Iran, during late March, were selected. The region was divided into 6 smaller areas (about 1.5×1.5 m^2), and plants in 3 areas irrigated with tap water were sampled as the control. In comparison, those in the other 3 areas were irrigated with wastewater and considered part of the wastewater treatment group. Simultaneous irrigation was carried out three times a week with the same volume of water and under the same conditions, for a period of three

months. After that, the control and treated plants were randomly selected and uprooted.

Analysis of the physical and chemical characteristics of the soil in the study area, as well as the heavy metal contents of the soil, tap water, and wastewater, are reported in Tables 1 and 2, respectively.

Table 1 Physical and chemical analysis of the soil

CEC Meq100 g^{-1} Soil	Texture	Silt %	Sand %	Clay %	T.N. %	O.C %	O.M. %	pH	EC (μs^{*} cm^{-1})
0.72	Loam	42.70	39.10	18.20	0.04	0.41	0.71	7.87	25.69

*µs = µSiemens

Table 2 Heavy metal contents of the tap water, wastewater, and soil

Heavy Metal	Tap water (ppb*)	Wastewater (ppb)	Soil (ppb)
As	0	0	778.71
Co	0.09	0.19	28.35
Ni	0.08	0.05	90.65
Zn	0.01	0.03	29.90
Cd	ND	ND	ND
Cu	0.008	0.01	15.25
Pb	0.03	0.03	2.20
Fe	0.02	0.39	17420.00

*: PPB is parts per billion

Morphological and anatomical studies: The plants in both control and wastewater treatment were observed weekly, and morphological characteristics such as the plants and leaves density, the plant and flower color, total biomass, the plant height, and the leaf and flower size were recorded. After three months of irrigation, the randomly selected plants were uprooted and their shoot and root organs were separated, divided into smaller sections, and fixed. The fixation process was carried out using Formaldehyde: Acetic acid: Ethanol (FAA) in a ratio of 2:1:17, followed by the next steps of the preparation process, including dehydration in ethanol and toluene, infiltration in paraffin and toluene, and embedding in paraffin (Ruzin, 1999). Then, the plant samples were subjected to serial sectioning (5-20 µm, depending on the type of tissue) by a rotatory microtome (MICROM HM 325). Next, Hematoxylin and Eosin (H&E) and methylene blue-Carmine alum staining (Ruzin, 1999) were used for histochemical examination, and the specimens were mounted in Entellan. A Nikon light research microscope (E200, Nikon, Tokyo, Japan) equipped with a digital camera (SAMSUNG SCB 2000) and Stereolite software (Stereolite, Shiraz University of Medical Sciences, Shiraz, Iran) was used for observation and photography.

Stereological studies for data validation - Stereolite software was used to convert the qualitative data into quantitative data, making them more reliable. For this reason, we employed the stereology method, selecting samples randomly and performing at least 40 repetitions for each attribute, such as diameter, thickness, length, width, and cell area. Then, the data obtained for each characteristic of the experimental group were quantitatively compared with those of the control group. The comparison of means was performed using Duncan's test at a 5% probability level, as determined by SAS software.

Results

Morphological characteristics - The halophyte *S. maritima* is a succulent plant that has a taproot system. Simple, entire-margin leaves were arranged in alternate phyllotaxy (Fig. 1). The dark green leaves were dense at early developmental stages. Over time, some changes in leaf morphology appeared. The color of the leaves faded, their density decreased, and they became smaller, so that the plants no longer looked fresh (Fig. 1B&C). Also, the stem took on different colors over time, varying from light to dark green and even dark purple. Florescence began in late August, when round bisexual flowers were

formed. The incomplete green flowers contained five petaloid sepals and five red stamens.

The wastewater-treated plants showed deviations earlier and more pronouncedly than the control, including changes in color and an aged appearance. The stems of the treated plants became more spaced over time, and their density decreased. Fluorescence in the treated plants began about 20 days later than in the control plants, and the flowers were smaller. The treated flowers were paler than the controls, and yellow flowers were rarely observed. The number of seeds in the wastewater-treated plant was lower and smaller than in the control.

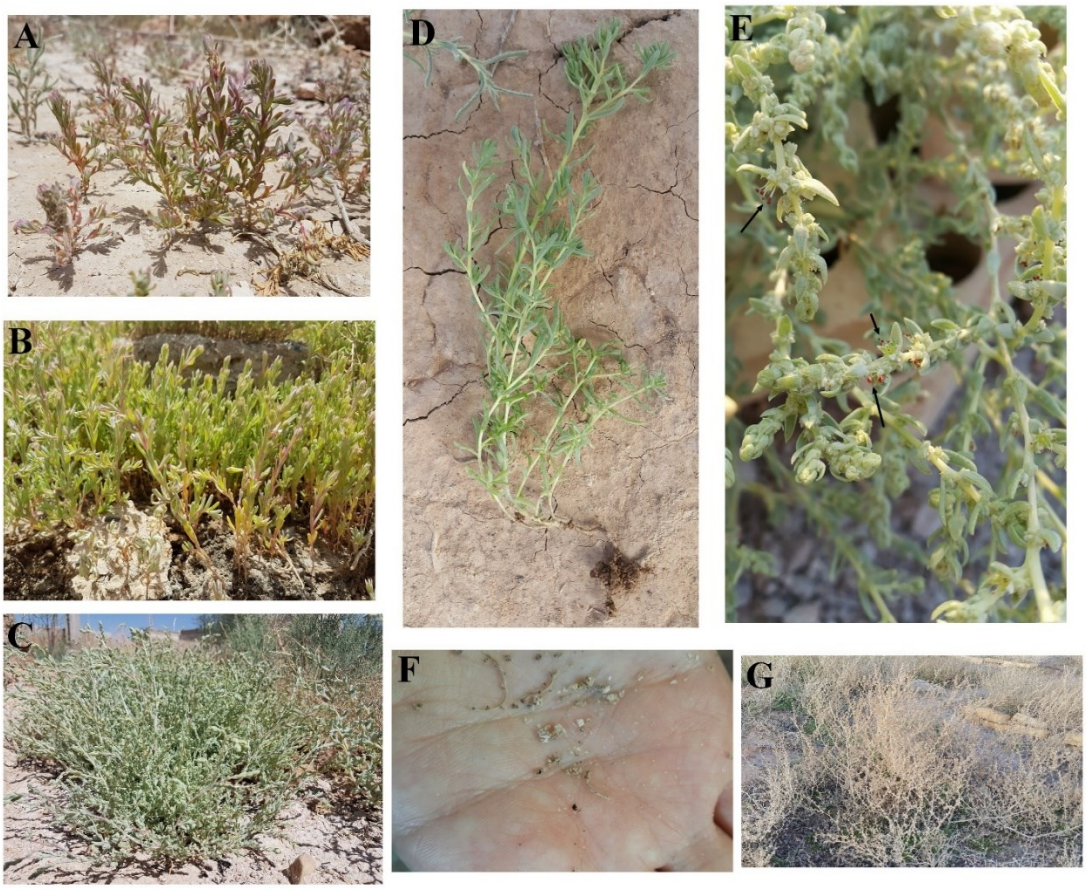

Fig. 1 Developmental stages of *Suaeda maritima* L. plants (control condition); **A** very young plants; **B** 30-day-old plants; **C** mature plants; **D** the tap root system; **E** a mature plant in the generative phase featuring incomplete tiny flowers with red stamens; **F** very small seeds of the plant; **G** the final stage of the plant development

Anatomical structure

The stem - In the control plants, the stem was covered with an outer layer of epidermis, beneath which there was a thick-walled collenchyma tissue (Fig. 2A). The remaining cortical space was occupied by the parenchymatic cells (Fig. 2B). These cells had a normal appearance early in the growth (Fig. 2B). Still, over time they changed and assumed very unusual wavy shapes of phellem cells showing some crests (Fig. 2C). Vascular cylinder displays the natural arrangement including the phloem on the top of the xylem, all on a discontinuous ring in the very young plants (Fig. 2A). The parenchymatic pith cells can be seen in the middle (Fig. 2A). During the late growth stages, the vascular arrangements changed and the phloem islands which spread regularly in the vascular cylinder, appeared. The islands were surrounded by the xylem and a large volume of the fiber cells (Figs. 2D, E, and F).

In plants treated with wastewater, the epidermal cells were thicker, and the cortical parenchymatic cells were larger than in the control. Also, there were some disruptions in the layers, which were more frequent in the treatment samples than in the control (Fig. 2E).

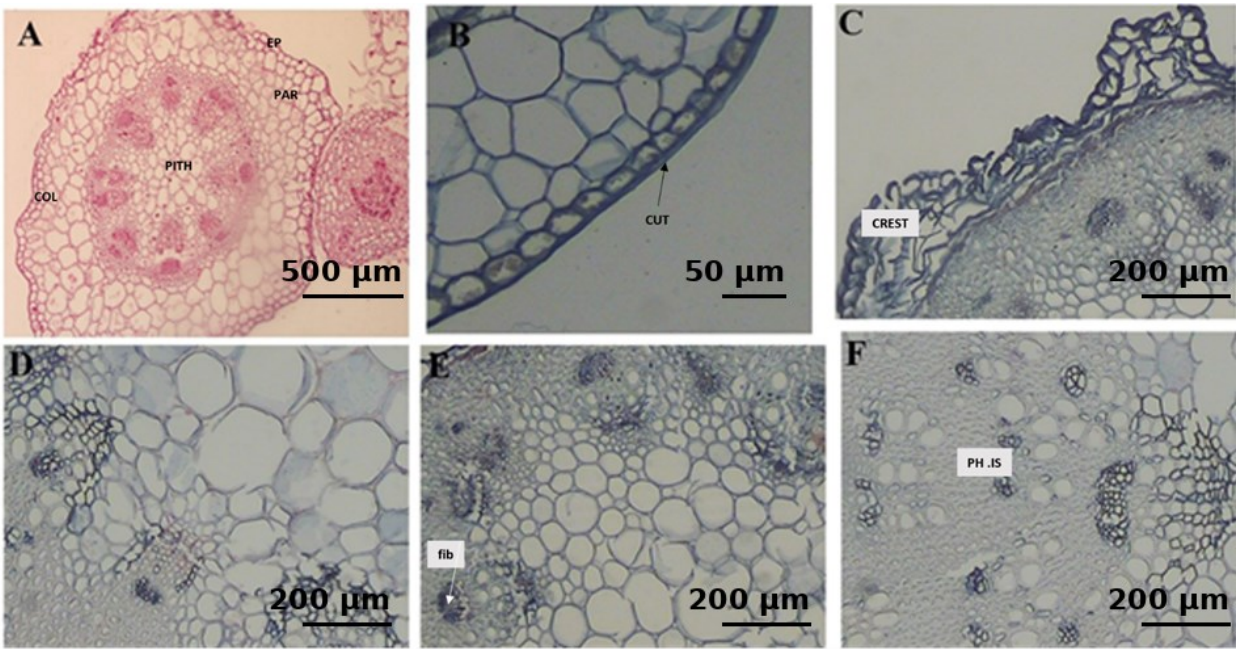

Fig. 2 The stem cross sections of *S. maritima* L.*;* **A** the general structure of the stem includes the epidermal, ground, and vascular systems (×4), and a young stem is being formed near the main stem; **B** the epidermis and cortex of the young control plant (×40); note the smooth surface of the epidermis and the regular parenchyma cortical cells as well as the thick cuticle outside the epidermal cells; **C** the mature control stem (×10); note the uneven epidermis and the deformed cortical cells; **D** the vascular cylinder in the control plant (×10); **E** the vascular cylinder in the treatment group (×10); **F** the phloem islands in the vascular cylinder of the mature control plant spread among numerous fiber cells and a number of xylem (×10). COL: collenchyma; EP: epidermis; PAR: parenchyma; PH.IS: phloem islands

The leaves - The small linear succulent leaves were in alternate arrangement (Fig. 1). The structure of the very young leaves represented three tissue systems (Fig. 3A). The outermost layer of the epidermal system was epidermis (Fig. 3A). On the young leaves, the common epidermal cells were almost regular, slightly extended, and had thick cuticle on the outside. There were a few stomata in both surface of the leaves (Fig. 3A). The well-ordered spongy parenchyma cells were located in the mesophyll (Fig. 3A). The mature leaves had a real uneven surface (Fig. 3B). The epidermal cells had a new form with peculiar shapes and were larger and covered with a thick cuticle layer (Figs. 3B and C). Sunken stomata (Fig. 3C), bulliform cells (Fig. 3C), simple straight trichomes (Fig. 3D), and secretory glands (Fig. 3F) were observed in the epidermis. The outer layer of mesophyll includes isodiametric small cells with large nuclei. The rest of the mesophyll consisted of both types of parenchyma, i.e., spongy and palisade (Fig. 3A, B, C, and E). There was a main vein right in the middle of the leaves, along with some smaller sub-veins (Fig. 3B).

In the mature leaves, the rugged epidermis featured large and sometimes giant cells, covered with a very thick cuticle (Fig. 3D). Sunken stomata and crypts, as well as simple unicellular/multicellular trichomes, and secretory glands were observed in the epidermal tissue (Figures 3D and E). The mesophyll comprises large, sometimes huge, spongy and palisade parenchyma with abnormal shapes. A big mid vein was located at the middle of the leaves, while other smaller veins were pinpointed at both ends (Fig. 3D). There were several trichomes on the outer side, which contributed to a more non-uniform appearance (Fig. 3D).

In the young leaves of the wastewater treatment group, epidermal cells were clearly extended, even showing wavy shapes (Fig. 3E). The cells in all layers of mature leaves were deformed and had less regulation (Fig. 3F). The cuticle in the treated leaf samples was thicker than the control (Figs. 3C and F).

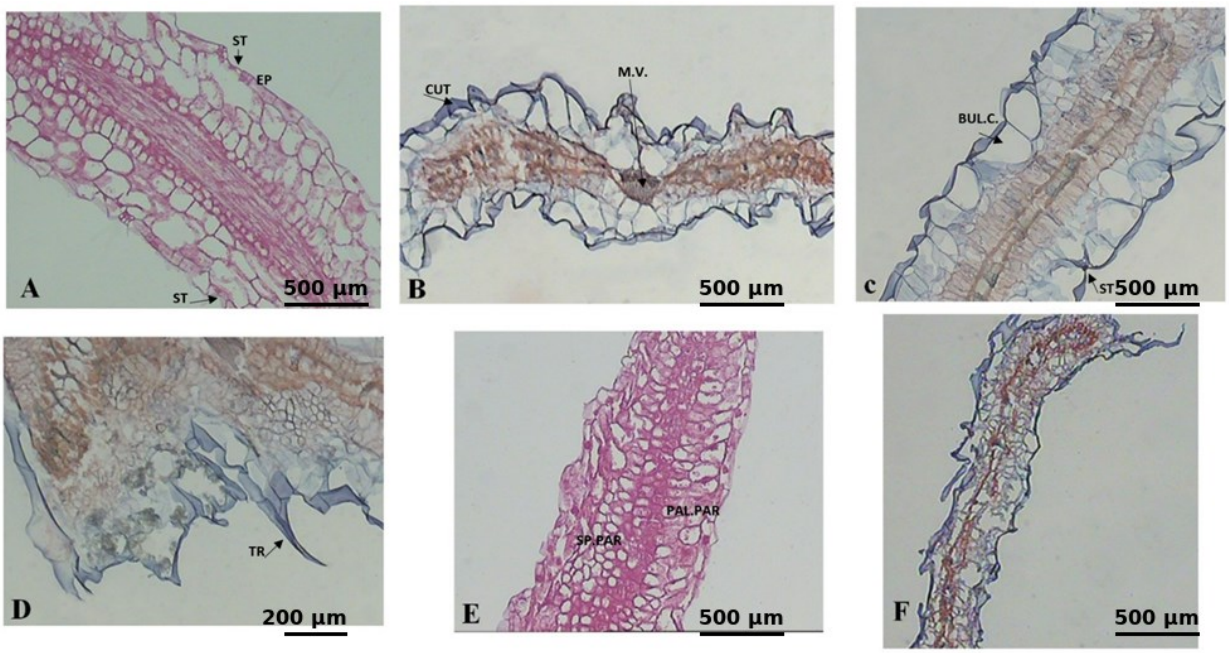

Fig. 3 *Suaeda maritima* leaf in control and the treated plants; **A** longitudinal section of the very young control leaf (×4): Note the regularity in the all layers and cells; **B** The appearance of mature leaf in control plants (×4): Note a mid-vein bundle at the middle of the leaf and lateral veins on the sides; **C** The leaf surface was really rugged, mature control leaf (×4): Note the thick cuticle, bulliform cells, and sunken stomata are detectable; **D** The mature control leaf (×10), Note the noticeable trichomes; **E** The treated young leaf (×4); **F** The treated mature leaf (×4) displaying completely deformed cells in tissue layers and thick cuticle on the outer surface. BUL.C: bulliform cell; CUT: cuticle; EP: epidermis; M.V: main vein; PAL. PAR: palisade parenchyma; SP.PAR: spongy parenchyma; ST: stomata; TR: trichome.

Fig. 4 The small flowers of *S. maritima* L. Dumort

The male reproductive organ - The very small green flower in the *S. maritima* was located compactly on the upper axis of the leaf (Fig. 4). These bisexual flowers, which were surrounded by several bracts that appeared at the end of summer. They had five green succulent tepals (petaloid sepals) and five stamens. Each stamen had a long filament and a big red anther (Fig.4). Two carpels were adjacent to each other. The plants are self-fertilizing and pollinated by wind.

The wastewater-treated plants that entered the reproductive phase later were smaller and paler in colour than the control. In addition, the seeds of plants grown from wastewater-treated seeds were fewer and smaller. The stamen had a long filament and a two-lobbed anther with four pollen sacs, as observed during early developmental stages in Fig. 5A. Each pollen sac included a large number of pollen grains (Figs. 5A-F). The mature pollen grains displayed cell wall ornamentation (Figs. 5G & H).

The anther comprised four structural layers (Fig. 5B). Its epidermis was the outermost layer, which ended in the fibrous (endothecium) layer. The transition (middle) layer comprised parenchyma cells in multilayers, and the tapetum layer, which directly enveloped the pollen sac. The tapetum layer included large cells with one or, occasionally, two large nuclei, which disappeared over time, since their role was pollen grain nutrition. These cells were of secretory type at first and later changed into plasmodial cells.

At early developmental stages, the pollen sac comprises undifferentiated archesporial cells (Fig. 5A), which later form the microspore mother cells (Fig. 5B). These cells were separated by the sac enlargement and underwent meiosis, after which the tetrad arose (Figs. 5C-E). Each tetrad matured to produce four microspores, which developed into pollen grains (Fig. 5F). The mature pollen grains included exine, intine, vegetative, and generative nuclei (Figs. 5G & H). At the late stage of development, and during dehiscence time, a fracture was created at the longitudinal end of the sac by the endothecium layer (Figs. 5I & J), whose location was recognized at the previous stage, i.e., stomium (Fig. 5F), where the mature pollens were released (Figs. 5K & L).

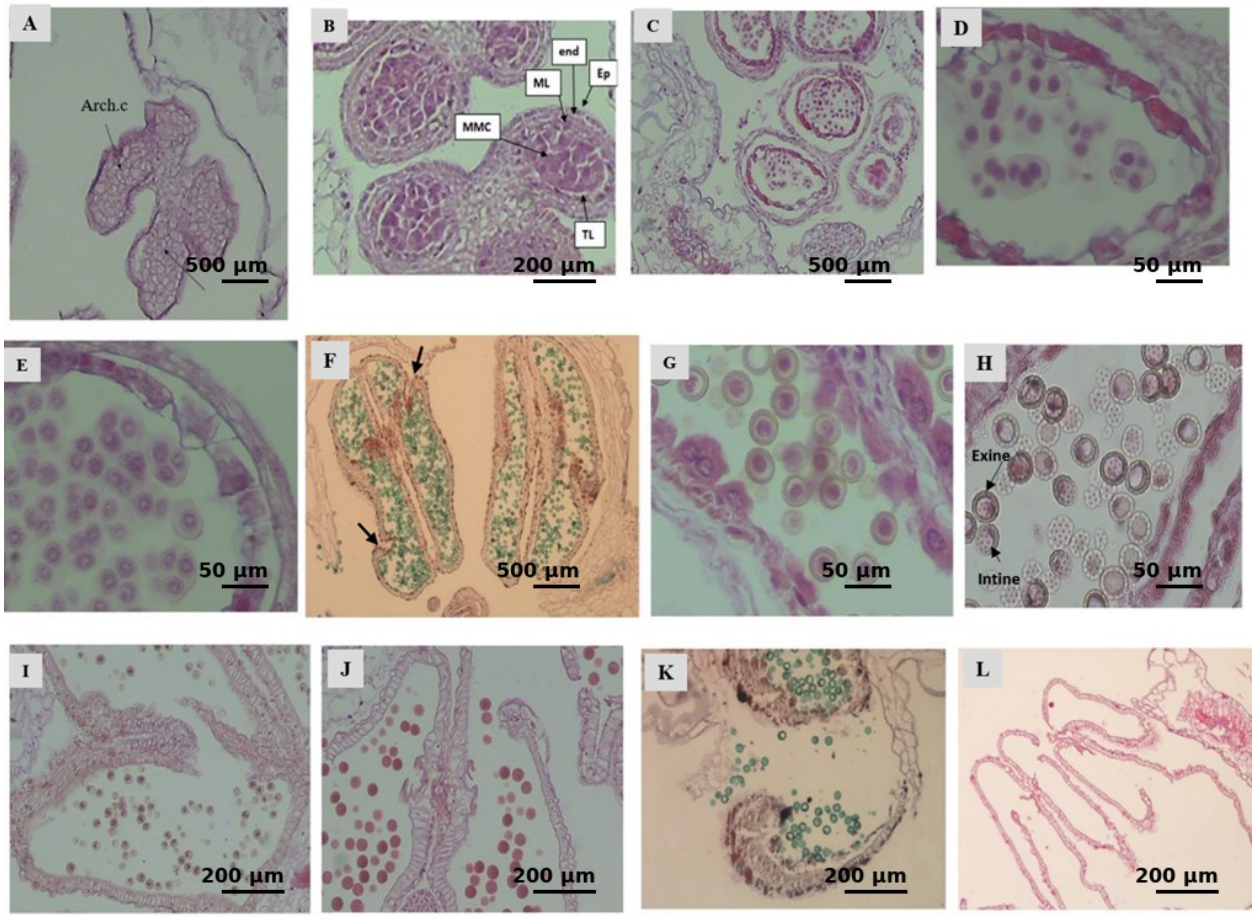

Fig. 5 Developmental stages of the male organ in *S. maritima L.* Dumort **A** very young anther with undifferentiated cells (×4); **B** different layers of the anther wall (×10); **C** Dyad and tetrad formation (×4), The transition layer were almost disappeared and the tapetum layer was separated from the others; **D** The tetrad formation (×40); **E** the tapetum cells were changing the shape (×40); **F** There were numerous young microspores in the pollen sac (×4): The arrows show the "stomium" location; **G** developing pollen grains (×40), The tapetum cells were noticeable with two nucleuses; **H** Mature pollen grains with outer ornamentation (×40); **I** The wall between two pollen sacs was degenerating (×10); **J** The release of pollen grains started with the gap at the longitudinal end of each pollen cavity. (×10); **K** the anther dehiscence (×10); **L** The empty pollen sac (×10), No pollen grains remained inside. Arch.c: archesporium cells; EP: Epidermis; end: endothecium; ML: Middle Layers; MMC: Microspore Mother Cell; TL: Tapetum Layer

The wastewater-irrigated plants produced smaller and fewer pollen grains than the control. Although most of the pollen grains from the control and treated plants were round, deformed shapes, especially crescent shapes, were more common in plants irrigated with wastewater. The fibrous layer of the endothecium was thinner in the treated plants than in the control. Moreover, the appearance of the sac fracture for releasing pollen grains occurred earlier than in the control. Figure 6 shows the comparison of control (Figs. 6A- C) and treated plants (Figs. 6D- F).

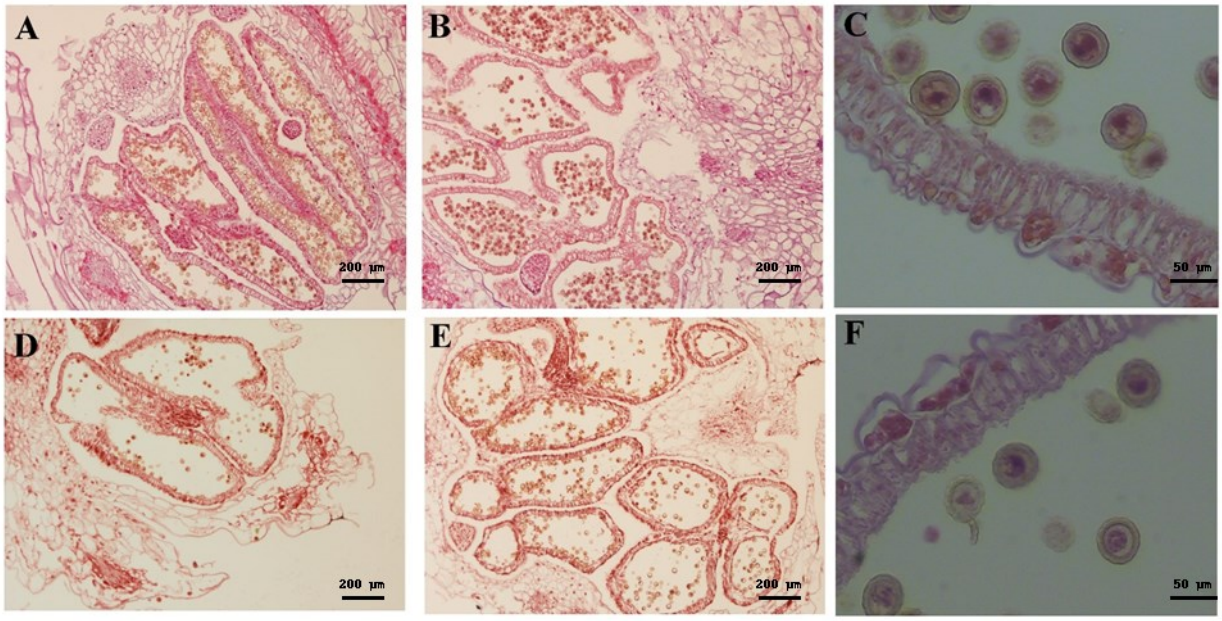

Fig. 6 Comparative anatomy of anther in *S. maritima* L. Dumort **A** (×10); **B** (×10); **C** (×40) illustrates the control plants, and **D** (×10); **E** (×10); **F** (×40) depict the wastewater-irrigated plants

Table 3 Stereological evaluation of anatomical characteristics of control and treated plants

Organ	Characteristic	Control (µm)	Treated Plant (µm)
Root	Cortical parenchyma area	552 b	3410 a
Root	Xylem vessel diameter	6.15 b	10.54 a
Stem	Cortical parenchyma area	1824 b	2826 a
Stem	Cortical parenchyma diameter	48.83 b	51.71 a
Stem	Epidermal cell area	314 b	715 a
Stem	Epidermal cell diameter	19.8 b	29 a
Leaves	Cuticular thickness	14 b	19 a
Flower	Endothecium layer thickness	21.1 a	17.3 b
Flower	Pollen grain diameter	16.7 a	9.4 a

Stereological evaluations — The stereological studies were performed using stereological software to confirm the quantitative microscopic observations. As shown in Table 3, there were differences between the control and treated *S. maritima* L. plants. The xylem vessel diameter and the cortical parenchyma area in the root of the treated plants increased as compared with the controls. In the stem sections, the cortical parenchyma area and its diameter, and the epidermal cell area and its diameter, increased in the treated plants compared with the control. In addition, the cuticular thickness of the leaves in the wastewater-irrigated samples was more than that of the control. In the anther of the treated plant, both the thickness of the fibrous layer and the diameter of the pollen grain decreased compared to the control. A comparison of means using Duncan's test at the 5% significance level in SAS software showed that the results were significant (Table 3).

Discussion

Vegetative structure - The young green stems of *Suaeda maritima* L. plants turned purple during development. Ebrahimi Nokande et al. (2022) also reported morphological changes in aloe vera plants due to industrial and urban pollution. The transverse sections of the stem demonstrated that the outer surface was not smooth and uniform and featured some crests. The epidermis was composed of one-layer cells covered with a thick cuticle on their outer surface. The cortex consisted of a layer of collenchyma and about three layers of parenchyma. The collenchyma cells were cube-shaped with thick cell walls. Our results are in line with those reported by Grigore et al. (2014)

for *Suaeda maritima* L. Previously, Essau (1988) reported the presence of nine crests on the outer surface of some Chenopodiaceae species, which are now classified as Amaranthaceae. Bercu and Bavaru (2004) also stated the same structure in *Salsola kali*. The stem of *Salsola crassa*, as reported by Mohammadi Jahromi et al. (2019b), had some crests on its outer surface, and other layers included palisade collenchyma and parenchyma, which joined the vascular cylinder. These findings are very similar to those from our study of the structure of *S. maritima* stems.

The spring branch number of *Suaeda salsa* received the highest score among all plant traits evaluated. A nonlinear relationship was observed between hydrological connectivity indices (HCIs) and plant traits, with the middle tidal flat being the most suitable for *S. salsa* growth. *S. salsa* adapts to different hydrological connectivity levels by forming distinct trait modules, with branch number playing a central role in this adaptation (Yu et al., 2023).

The vascular cylinder, which was larger than the cortex, began with a multilayer pericycle and consisted of small cells. In the young sections, the vascular system consisted of phloem above the xylem, and a cap of thick-walled, cell-rich fibers on the upper side of the phloem. By maturation, very thickened lignified sclerenchyma cells were formed, whereas the xylem was lignified with less thickness. This finding aligns with that of Grigore et al. (2014), who reported phloem islands among xylem elements in aged sections surrounded by sclerified cells. Additionally, they noted that the xylem elements were very thick and contained low lignin.

The treated stems showed a more irregular and uneven epidermis than the control. Parenchyma cells in both the cortex and pith were larger than the control and had unusual shapes. There were some ruptures in the cortex and vascular cylinder. Studies have identified deformed cells in response to certain heavy metals (Shah et al., 2010; Kouhi et al., 2016). For example, large, irregular cells, especially in the cortex, and ruptures in tissue layers resulting from heavy metal pollution have been reported in *Salsola crassa* (Mohammadi Jahromi et al., 2019b). In another study, *Potamogeton* L. plants exposed to Cu and Ag showed structural changes in their stems. Likewise, Al-Saadi (2013) found in their research that the size, arrangement, and shape of the parenchyma in the cortex changed, and that the cortical intercellular spaces widened, indicating a decrease in the number of vascular bundles. In another research study on *Cicer arietinum* treated with Cr, ultrastructural deformation and some other changes in the root were reported (Medda & Mondal, 2017). Heavy metals can affect homeostasis in plants, such as water uptake, transpiration, and nutrient metabolism (Poschenrieder & Barcelo, 2004). They can also interfere with gated ion channels (Demidchik, 2018), thereby affecting plant anatomy. For instance, Al toxicity inhibits root elongation by damaging the root apex (Zheng, 2010), thereby restricting water and mineral uptake. Moreover, Al can form electrostatic bonds with oxygen-donor ligands, preferably on the outer surface of the plasma membrane and on cell wall pectin (Yamamoto et al., 2001). The binding of Al to bio membranes can lead to rigidification (Jones et al., 2006).

The alternate succulent leaves of *Suaeda maritima* L. Dumort. showed three tissue systems: epidermal, ground, and vascular. The epidermal tissue is composed of compact common epidermal cells with some stomata, bulliform cells, and a thick cuticle. The spongy and palisade parenchyma cells were arranged regularly in the mesophyll. The vascular system encompasses the mid vein and the lateral veins. Toderich et al. (2010) recognized swollen epidermal cells, hypodermal cells, and water-bearing parenchyma cells in the structure of *Salsola*'s bracts. Grigore et al. (2014) identified two specific palisade layers and an isodiametric cell layer behind the epidermis of *Petrosimonia oppositifolia* in the Chenopodiaceae, which play a role in photosynthesis. This structure has also been reported in the leaves of *Salsola kali* and other halophytes (Bercu & Bavaru, 2004; Grigore et al., 2014).

The leaves of *S. maritima* exposed to wastewater treatment showed structural changes. The cells in all tissue layers exhibited more irregularities and deformed shapes, and were larger than those in the control. The reformed traits are attributed to the adverse effects of the pollution, especially with heavy metals. Gomes et al. (2011) stated that the impact of heavy metals are on plant hormones. They change the plant's hormonal balance, such as a decrease in endogenous auxins, which is a response to As (Bücker-Neto et al., 2017), leading to morphological and structural changes, e.g., in size and shape. Occurrence of the structural changes in the roots, stems, and leaves of many plants in response to heavy metals, as stated in Yadav et al.

(2021) and Ghukwu and Gulser (2025), as well, which were consistent with our results.

The male generative organ - The *S. maritima* small flowers are bisexual, and the male generative organ is composed of five filamentous red stamens. The treated plants entered the generative phase later and produced smaller flowers than the control. The treated seeds were also less abundant and smaller. The characteristics of the flowers we observed were similar to those of heavy metal-treated *Salsola crassa* flowers reported by Mohammadi Jahromi et al. (2019b). They stated that treating the plants with wastewater containing heavy metals results in structural changes, as well as a decrease in the frequency and size of flowers and seeds. The general anatomy of *S. maritima* flowers in our study is also similar to that of *Salsola kali* (Idzikowska, 2005).

The scrutiny of anther sections revealed that the outer layer consisted of epidermis with compact cells, followed by a fibrous layer and a transition layer. The inner layer was the tapetum, comprising big, elongated cells with one or two nuclei, which fed the pollen grains via secretory and plasmodial processes. The latest layer surrounded the pollen sac, which contained numerous pollen grains.

During microsporogenesis, the nucleus of each microspore mother cell underwent meiosis, leading to the formation of a tetrad (four haploid cells) that later divided, producing four distinct haploid microspores. The young microspores underwent morphological and structural changes, ultimately forming mature pollen grains that dispersed at late developmental stages. The male generative organs of *S. maritima* in this study are similar to those of *S. kali* as described by Idzikowska (2005).

In the treated samples, the number and size of pollen grains in the pollen sac decreased compared to the control. The shape of the pollen grains changed over time, from almost round to deformed shapes, such as crescents. The observed abnormalities in the pollen sac sections of the wastewater treatment group were more frequent than in the control, and ruptures occurred sooner. Changes in the tissues of generative organs as observed in this study are generally in line with the findings of the literature on the effects of heavy metal contamination on plants (Yousefi et al., 2010)

The stereological studies - The stereological-based evaluation confirms the quantitative results of this study. In roots, the diameter of the xylem vessels and the area of the cortical parenchyma increased under wastewater treatments compared to the control. In the stem, the cortical parenchyma area and diameter, in addition to the epidermal cell area and diameter, all increased in the treated sections. Moreover, the treated leaves exhibited a decrease in cuticular thickness. Additionally, the thickness of the fibrous layer and the diameter of pollen grains decreased in the treated samples.

Studies reveal that different pollutants may differentially affect various aspects of plants, including morphology, anatomy, and physiology. For instance, heavy metal contaminants in the air affect leaf structure, causing an increase in leaf stomatal density per area, a decrease in stomatal size, a reduction of parenchyma cells in the mesophyll, and an increase in the thickness of the outer wall of epidermal cells to prevent the pollutants from entering them (Gostin, 2009).

Keyster et al. (2020) reported that heavy metal accumulation in plant cells often leads to cellular impairment and senescence. The apoplastic space around cells is significant for the uptake of heavy metals. In the cell wall, pectin senses heavy metals and transduces wall signals, as well as signals from plasma membrane receptors, triggering an appropriate defence strategy. Heavy metals move into the root apoplastic space by unwanted bulk flow and follow the apoplastic pathway, which stops in the Casparian strips, or move through the plasma membrane into the symplastic space using protein carriers and pumps, acting as receptors or sensors (Keyster et al., 2020).

Suaeda maritima reduces its biomass as an energy-conservation strategy to survive under heavy-metal stress. The plant efficiently scavenges reactive oxygen species by increasing the expression of antioxidative enzymes. Under cadmium and lead stress, Suaeda maritima up-regulates various metabolites, including sugars, amino acids, and polyphenols, which may help with osmotic balance, ionic homeostasis, and ROS scavenging for stress tolerance (Fatnani & Parida, 2024).

Plants do not have an inflow channel for the unnecessary heavy metal Pb, but it is trapped by the root surface (Sharma & Dubey, 2005). It can be present in root tissues at high levels via unknown mechanisms, then translocated to the

shoot, causing lethal effects on plant growth, morphology, and physiology. This element can bind to enzymes' sulfhydryl groups, rendering them inactive (Pirzadah et al., 2019). At high concentrations, Pb arrests seedling growth, decreases leaf chlorophyll content, deforms chlorophyll, and disrupts nuclear integrity (Zhou et al., 2018). Zarinkamar et al. (2013) reported that different Pb concentrations in Matricaria chamomilla did not induce significant morphological changes at various developmental stages, except for a reduction in total biomass. Gomes et al. (2011) revealed that heavy metal pollution in Brachiaria decumbens increased the thickness of the exodermis and endodermis layers in the root, as well as the thickness of the xylem and cortical parenchyma walls. Zn was also found to decrease the photosynthesis rate via its effect on the chloroplast structure (Azzarello et al., 2012). Furthermore, Hg^{2+} and Cd^{2+}caused deformation in the stem vascular bundles and in xylem and phloem, respectively (Gupta & Chakrabarti, 2013). Al deflected plant growth and development, inhibited root and shoot elongation, and led to a decrease in biomass production (Parizadah et al., 2019).

Conclusion

In this research, we found that the halophyte *Suaeda maritima* can tolerate very severe environmental conditions, but it undergoes some morphological and structural changes in almost all tissues and cells. The size and number of leaves and flowers of the plants treated with wastewater containing heavy metals decreased. Moreover, the flowers' dehiscence occurred earlier due to a thinner fibrous layer in the treated anthers. This suggests that the pollen grains that spread in the environment are probably inefficient. Structurally, in wastewater-treated samples, the cells showed deformation and size changes. Also, the cell walls were almost thicker, the size of parenchyma cells and xylem diameter were larger, the cuticle thickness was greater, and the layer showed irregularities. These changes reveal that the plant is resisting the stress conditions of wastewater and its heavy metal pollutants. For instance, a thicker cell wall can bind more heavy metals and inhibit their translocation to higher organs. The larger xylem can help pump water upward with great force, and larger parenchyma cells help keep heavy metals in the vacuole and prevent their movement in the plant. Finally, the plant underwent morphological and anatomical changes to adapt to the adverse conditions and survive.

References

Al-Saadi, A. A. M. (2013). The effect of some heavy metals accumulation on physiological and anatomical characteristic of some *Potamogeton* L. plant. *International Journal of Ecology and Environmental Sciences*, *4*(1), 100-108. http://www.bioinfopublication.org/viewhtml.php?artid=BIA0001927

Azzarello, E., Pandolfi, C., Giordano, C., Rossi, M., Mugnai, S., & Mancuso, S. (2012). Ultramorphological and physiological modifications induced by high zinc levels in *Paulownia tomentosa*. *Environmental and Experimental Botany, 81,* 11-17. https://doi.org/10.1016/j.envexpbot.2012.02.008

Bercu, R., & Bavaru, E. (2004). Anatomical aspects of *Salsola kali* subsp. Ruthenica (Chenopodiaceae). *Phytologia Balcananica*, *10* (2-3), 227-232. http://www.bio.bas.bg/~phytolbalcan/PDF/10_2-3/10_2-3_16_Bercu_&_Bavaru.pdf

Bücker-Neto, L., Paiva, A.L.S., Machado, R.D., Arenhart, R.A., & Margis-Pinheiro, M. (2017). Interactions between plant hormones and heavy metals responses. *Genetics and Molecular Biology, 40*(Suppl 1), 373–386. https://doi.org/10.1590/1678-4685-GMB-2016-0087

Butnik, A.A., Japakova. U.N., & Begbaeva, G.F. (2001). Halophytes: structure and adaptation. In S. W. Breckle, M. Veste & W. Wucherer (Eds). *Sustainable Land Use in Deserts* (pp. 147-153). Springer. https://doi.org/10.1007/978-3-642-59560-8_15

Debez, A., Saadaoui, D., Ramani, B., Ouerghi, Z., Koyro, H.W., Huchzermeyer, B., & Abdelly, C. (2006). Leaf H^{+}-ATPase activity and photosynthetic capacity of *Cakile maritima* under increasing salinity. *Environmental and Experimental Botany*, *57*(3), 285–295. https://doi.org/10.1016/j.envexpbot.2005.06.009

Demidchik, V. (2018). ROS-Activated ion channels in plants: biophysical characteristics, physiological functions and molecular nature. *International Journal of Molecular Sciences*, *19*(4), 1263-1281. https://doi.org/10.3390/ijms19041263

Ebrahimi Nokande, S., Razavi, S. M., & Afshar Mohammadian, M. (2022). Some morphological and physiological characteristics of Aloe vera under the treatment of urban and industrial wastewater. *Journal of Plant Biological Sciences*, *14*(1), 1-16. https://doi.org/10.22108/ijpb.2022.134064.1291 [In Persian]

Essau, K. (1988). *Plant anatomy*. John Wiley & Sons.

Fatnani, D., Patel, M., & Parida, A.K. (2023). Regulation of chromium translocation to shoot and physiological, metabolomic, and ionomic adjustments confer chromium stress tolerance in the halophyte *Suaeda maritima*. *Environmental Pollution*, *320*, 121046 https://doi.org/10.1016/j.envpol.2023.121046

Fatnani, D., & Parida, A.K. (2024). Unravelling the halophyte *Suaeda maritima* as an efficient candidate for phytostabilization of cadmium and lead: Implications from physiological, ionomic, and metabolomic responses. *Plant Physiology and Biochemistry, 212*, 108770. https://doi.org/10.1016/j.plaphy.2024.108770

Ghukwu, E.Ch., & Gulser, C. (2025). Morphological, physiological, and anatomical effects of heavy metals on soil and plant health and possible remediation technologies. *Soil Security*, *18*, 100178. https://doi.org/10.1016/j.soisec.2025.100178

Gomes, M.P., de Sá e Melo Marques, T.C.L.L., de Oliveira Gonçalves Nogueira, M., de Castro, E.M., & Soares, Â.M. (2011). Ecophysiological and anatomical changes due to uptake and accumulation of heavy metal in *Brachiaria decumbens*. *Scientia Agricola, 68*(5), 566–573. https://doi.org/10.1590/S0103-90162011000500009

Gostin, I.N. (2009). Air pollution effects on the leaf structure of some Fabaceae species. *Notulae Botanicae Horti Agrobotanici Cluj-Napoca*, *37*(2), 57-63. https://doi.org/10.15835/nbha3723078

Grigore, M.N., Ivanescu, L., & Toma, C. (2014). Chenopodiaceae. In *Halophytes: an integrative anatomical study*. Springer. https://doi.org/10.1007/978-3-319-05729-3_8

Gupta, S., & Chakrabarti, S.K. (2013). Effect of heavy metals on different anatomical structures of *Bruguiera sexangula*. *International Journal of Bio-resource and Stress Management*, *4*(4), 605-609. https://www.cabidigitallibrary.org/doi/full/10.5555/20143114442

Hameed, M., Ashraf, M., Ahmad, M.S.A., & Naz, N. (2010). Structural and Functional Adaptations in Plants for Salinity Tolerance. In M. Ashraf, M. Ozturk, & M. Ahmad, M. (eds). *Plant Adaptation and Phytoremediation*. Springer. https://doi.org/10.1007/978-90-481-9370-7_8

Hu, Zh., Zhao, C., Li, Q., Feng, Y., Zhang, X., Lu, Y., ... & Ji, W. (2023). Heavy Metals Can Affect Plant Morphology and Limit Plant Growth and Photosynthesis Processes. *Agronomy*, *13*(10), 2601. https://doi.org/10.3390/agronomy13102601

Idzikowska, K. (2005). Morphological and anatomical structure of generative organs of *Salsola kali* spp. Ruthenica (Iljin) Soo at the SEM level. *Acta Societatis Botanicorum Poloniae*, *74*(2), 99-109. https://doi.org/10.5586/asbp.2005.014

Jesus, D.d.S., Martins, F.M., & Azevedo Neto, A.D. (2016). Structural changes in leaves and roots are anatomical markers of aluminum sensitivity in sunflower. *Pesquisa Agropecuaria Tropical*, *46*(4), 383-390. https://doi.org/10.1590/1983-40632016v4641426

Jones, D.L., Blancaflor, E.B., Kochian, L.V., & Gilroy, S. (2006). Spatial coordination of aluminum uptake, production of reactive oxygen species, callose production and wall rigidification in maize roots. *Plant Cell and Environment, 29*(7), 1309-1318. https://doi.org/10.1111/j.1365-3040.2006.01509.x

Keyster, M., Niekerk, L.A., Basson, G., Carelse, M., Bakare, O., Ludidi, N., ... & Gokul, A. (2020). Decoding heavy metal stress signaling in plants: Towards improved food security and safety. *Plants*, *9*(12), 1781. https://doi.org/10.3390/plants9121781

Kouhi, S.M.M., Lahouti, M., Ganjeali, A., & Entezari, M.H. (2016). Anatomical and ultrastructural responses of *Brassica napus* after long-term exposure to excess zinc. *Turkish Journal of Biology*, *40*(3), 652-660. https://doi.org/10.3906/biy-1411-13

Koyro, H.W. (2002). Ultrastructural effects of salinity in higher plants. In A. Läuchli, & U. Lüttge (Eds.). *Salinity: Environment, Plants, Molecules* (pp. 139–158). Springer. https://link.springer.com/book/10.1007/0-306-48155-3#page=148

Koyro, H.W., Geissler, N., Hussin, S., Debez, A., & Huchzermeyer, B. (2008). 5 Strategies of halophytes to survive in a salty environment. In N. A. Khan & S. Singh (Eds.), *Abiotic stress and plant responses* (pp 83-104). IK International Publishing House. https://B2n.ir/nm3648

Marschner, H, (1995). *Mineral nutrition of higher plants*. Academic Press.

Medda, S.h., & Mondal, N.K. (2017). Chromium toxicity and ultrastructural deformation of *Cicer arietinum* with special reference of root elongation and coleoptile growth. *Annals of Agricultural sciences*, *15*(3), 396-401. https://doi.org/10.1016/j.aasci.2017.05.022

Megdiche, W., Ben Amor, N., Debez, A., Hessini, K., Ksouri, R., Zuily-Fodil, Y., & Abdelly, C. (2007). Salt tolerance of the annual halophyte *Cakile maritima* as affected by the provenance and the developmental stage. *Acta Physiologiae Plantarum, 29,* 375-384. https://doi.org/10.1007/s11738-007-0047-0

Mohammadi Jahromi, N.S., Jonoubi, P., Majd, A., & Dehghani, M. (2019 a). Root structural changes of two remediator plants as the first defective barrier against industrial pollution and their hyperaccumulation ability. *Environmental Monitoring and Assessment, 191*(3), 148. https://doi.org/10.1007/s10661-019-7240-7

Mohammadi Jahromi, N.S., Jonoubi, P., Majd, A., & Dehghani, M. (2019 b). Investigating the anatomy of the halophyte *Salsola crassa* and the impact of industrial wastewater on its vegetative and generative structures. *Turkish Journal of Botany*, *43*(6), 785-797. https://doi.org/10.3906/bot-1812-46

Pandey, A.K., Zoric, L., Sun, T., Karanović, D., Fang, P., Borišev, M., ... & Xu, P. (2022). The anatomical basis of heavy metal responses in legumes and their impact on plant-rhezosphere interaction. *Plants*, *11*(19), 2554. https://doi.org/10.3390/plants11192554

Parida, A.K., Veerabathini, S.K., Kumari, A., & Agarwal, P.K. (2016). Physiological, anatomical and metabolic implications of salt tolerance in the halophyte *Salvadora persica* under hydroponic culture condition. *Frontiers in Plant Sciences*, 7, 351. https://doi.org/10.3389/fpls.2016.00351

Parizadah, T.B., Malik, B., Salam, Sh.T., Ahmad Dar, P., & Rashid, S. (2019). Impact of heavy metal stress on plants and the role of various defense elements. *Iranian Journal of Plant Physiology, 9*(4), 2883-2900. https://sanad.iau.ir/Journal/ijpp/Article/1025567

Petrovic, D., Krivokapic, S., Anascov, G.T., & Lucovic J. (2021). Effect of heavy metals on stem anatomical characteristics of *Trapa natans* L. from Skadar lake (Montenegro). *Bioscience Journal*, *37*, e37083. https://doi.org/10.14393/BJ-v37n0a2021-54073

Poschenrieder, C., & Barcelo, J. (2004). Water relations in heavy metal stressed plants. In M. N. V. Prasad (Ed.), *Heavy Metal Stress in Plants* (pp. 249–270). Springer. https://doi.org/10.1007/978-3-662-07745-0_10

Ruzin, S.E. (1999). *Plant microtechnique and microscopy*. Oxford University Press.

Shah, F.U.R., Ahmad, N., Masood, K.h.R., Peralta-Videa, J.R., & Ahmad, F.D. (2010). Heavy Metal Toxicity in Plants. In M. Ashraf, M. Ozturk, & M. S. A. Ahmad (Eds.), *Plant Adaptation and Phytoremediation. Heidelberg* (pp. 71-97). Springer.

https://doi.org/10.1007/978-90-481-9370-7_4

Sharma, P., & Dubey, R.S. (2005). Lead toxicity in plants. *Brazilian Journal of Plant Physiology*, *17*(1), 35–52. https://doi.org/10.1590/S1677-04202005000100004

Toderich, K.N., Shuyskaya, E.V., Khujanazarov, T.M., Ismail, Sh., & Kawabata, Y. (2010). The structural and functional characteristics of Asiatic desert halophytes for phytostabilization of polluted Sites. In M. Ashraf, M. Ozturk, & M. S. A. Ahmad (Eds.), *Plant Adaptation and Phytoremediation* (pp. 245-274). Springer. https://doi.org/10.1007/978-90-481-9370-7_12

Wang, S.M., Zhang, J.L., & Flowers, T.J. (2007). Low affinity Na^+ uptake in the halophyte *Suaeda maritima*. *Plant Physiology*, *145*(2), 559-571. https://doi.org/10.1104/pp.107.104315

Wang, X., Shao, X., Zhang, W., Sun, T., Ding, Y., Lin, Z. & Li, Y. (2022). Genus *Suaeda*: Advances in phytology, chemistry, pharmacology and clinical application (1895 – 2021). *Plant Physiology*, *179*, 106203 https://doi.org/10.1016/j.phrs. 2022.106203

Yamamoto, Y., Kobayashi, Y., & Matsumoto, H. (2001). Lipid peroxidation is an early symptom triggered by aluminum, but not the primary cause of elongation inhibition in Pea roots. *Plant Physiology*, *125*(1), 199-208. https://doi.org/10.1104/pp.125.1.199

Yadav, V., Arif, N., Kováč, J., Singh, V.P., Tripathi, K.D., Chauhan, D. K., & Vaculík, M. (2021). Structural modifications of plant organs and tissues by metals and metalloids in the environment: A review. *Plant Physiology and Biochemistry*, *159*, 100-112. https://doi.org/10.1016/j.plaphy.2020.11.047

Yousefi, N., Chehregani, A., Malayeri, B., Lorestani, B. & Cheraghi, M. (2010). Investigating the effect of heavy metals on developmental stages of anther and pollen in Chenopodium botrys L. (Chenopodiaceae). *Biological Trace Element Research*, *140*(3), 368-376. https://doi.org/10.1007/s12011-010-8701-6

Yu, Z., Huang, L., Bai, J., Zhang, G., Wang, W., Wang, D., Wang, C., Wang, Y., Chen, G. & Liu, Z. (2023). Seasonal response of *Suaeda salsa* to hydrological connectivity in intertidal salt marshes through changing trait networks. *CATENA*, *222*, 106857. https://doi.org/10.1016/j.catena.2022.106857

Zarinkamar, F., Saderi, Z. & Soleimanpour, S. (2013). Excluder strategies in response to Pb toxicity in *Matricaria Chamomilla*. *Advances in Bioresearch*, *4*(3), 39-49. http://www.soeagra.com/abr/abrsept_2013/8.pdf

Zhang, D., Tian, Ch, & Mai, W. (2024). Exogenous sodium and calcium alleviate drought stress by promoting the succulence of *Suaeda salsa*. *Plants, 13*(5), 721. https://doi.org/10.3390/plants13050721

Zheng, S.J. (2010). Crop production on acidic soils: overcoming aluminum toxicity and phosphorus deficiency. *Analls of Botany*, *106*(1), 183– 184. https://doi.org/10.1093/aob/mcq134

Zhou, J., Zhang, Z., Zhang, Y., Wei, Y., & Jiang, Z. (2018). Effects of lead stress on the growth, physiology, and cellular structure of privet seedlings. *PLOS One*, *13*(3), e0191139. https://doi.org/10.1371/journal.pone.0191139